Journal of Non-Crystalline Solids 356 (2010) 2465–2467

Contents lists available at ScienceDirect

Journal of Non-Crystalline Solids

journal homepage: www.elsevier.com/ locate/ jnoncrysol

Influence of the temperature on the nucleation of silver nanoparticles in Tm^{3+}/Yb^{3+} codoped $PbO–GeO_2$ glasses

T.A.A. de Assumpção [a], D.M. da Silva [a], L.R.P. Kassab [b], J.R. Martinelli [c,*], C.B. de Araújo [d]

[a] Departamento de Engenharia de Sistemas Eletrônicos, EPUSP, Brazil
[b] Laboratório de Vidros e Datação – FATEC-SP, CEETEPS/UNESP, Brazil
[c] Centro de Ciências e Tecnologia de Materiais – IPEN-SP, Brazil
[d] Departamento de Física, Universidade Federal de Pernambuco, 50670-901 Recife, PE, Brazil

ARTICLE INFO

Article history:
Received 15 October 2009
Received in revised form 30 December 2009
Available online 11 June 2010

Keywords:
Nanoparticles;
Upconversion;
Lead germanate glass

ABSTRACT

The influence of the temperature on the nucleation of silver nanoparticles (NPs) in Tm^{3+}/Yb^{3+} codoped $PbO–GeO_2$ glasses was studied in this work. The infrared-to-visible frequency upconversion (UC) luminescence of Tm^{3+} ions was used to probe the NPs nucleation and the results were correlated with the increase of the heat-treatment temperature. Emission spectra in the blue–red region were measured by exciting the samples with a cw 980 nm diode laser in resonance with the Yb^{3+} transition ($^2F_{7/2} \rightarrow {}^2F_{5/2}$). The results were correlated with transmission electron microscopy measurements and revealed the different behavior of the nucleation process as a function of temperature. The enhanced UC emission in the visible region is attributed to the increased local field in the proximity of the silver NPs combined with the $Yb^{3+} \rightarrow Tm^{3+}$ energy transfer.

1. Introduction

The control of nucleation processes of nanocrystals is of great interest because new characteristics of materials can be obtained. In the case of solids, optical, mechanical, magnetic, and electric properties can be modified, some of them even improved [1–3]. The nucleation and growth of quantum dots [4], and the exploitation of plasmonic effects in metallic nanoparticles (NPs) are examples of photonic applications of current interest [1,2,5–7]. In the case of metallic NPs several methods have been reported in the literature such as the use of electron beam, femtosecond laser, ultra-violet irradiation, and heat-treatment [7–13].

In this paper, we report the influence of heat-treatment temperature (T_{ht}) on the nucleation of silver NPs in germanate glass. The aim of this work is to investigate the best way to heat-treat samples, considering that the luminescence efficiency of rare-earth ions (REI) may be enhanced through energy transfer (ET) between metallic NPs and rare-earth ions (REI) and/or by the enhancement of local field effect in the proximity of the NPs.

Germanate glasses are very good candidates for these studies because they exhibit large transmittance window (from the visible to the infrared region), low cutoff phonon energy, high refractive index, and large chemical stability.

The nucleation of silver and gold NPs in germanate glasses was recently reported [14] and the enhancement of the REI luminescence in $PbO–GeO_2$ (PGO) glass containing silver NPs was reported for samples doped with Pr^{3+} [15], Er^{3+} [16], and Er^{3+}/Yb^{3+} [17]. The influence of gold NPs in Eu^{3+} doped germanate glasses was reported in ref. [18]. On the other hand near-infrared third-order nonlinearity of PGO films containing Cu and Cu_2O NPs indicated a large potential for all-optical switching [19]. More recently the enhancement of the infrared-to-visible upconversion (UC) process in Tm^{3+}/Yb^{3+} codoped PGO glass containing silver NPs was also reported [20].

2. Experimental procedure

Glasses were prepared with composition $59PbO–41GeO_2$ (wt.%), following the melting-quenching procedure. The glasses were doped with 0.5 Tm_2O_3, 2.0 Yb_2O_3, and 3.0 $AgNO_3$ (wt.%). The reagents were melted at 1200 °C in an alumina crucible for 1 h and homogenized with a quartz stick, quenched in a pre-heated brass mold, annealed at 420 °C for 1 h, and cooled to room temperature inside a furnace to avoid internal stresses. Glass samples were polished and heat-treated for different temperatures in order to reduce Ag^+ to Ag^0 and to nucleate silver NPs. The samples were heat-treated for 6 h, continuously, at the following temperatures: 380, 420, 460, 480, 500, 520, and 540 °C.

Optical absorption was measured with a commercial spectrophotometer, and luminescence was measured exciting the samples with a cw diode laser operating at 980 nm in resonance with Yb transition ($^2F_{7/2} \rightarrow {}^2F_{5/2}$). UC luminescence was observed in the blue–red region (425–700 nm) and analyzed using a spectrometer equipped with a photomultiplier.

* Corresponding author.
E-mail addresses: thiago_blade@hotmail.com (T.A.A. de Assumpção), kassablm@osite.com.br (L.R.P. Kassab), jroberto@ipen.br (J.R. Martinelli).

0022-3093/$ – see front matter © 2010 Elsevier B.V. All rights reserved.
doi:10.1016/j.jnoncrysol.2010.02.016

A 200 kV transmission electron microscope (TEM) was used to investigate the size distribution and the shape of the nucleated silver NPs. Glass samples were ground down to powder, mixed to distilled water, and partially decanted. The floating part was taken by using an appropriated sample holder (metallic screen) and analyzed by TEM.

Energy dispersive X-ray spectroscopy (EDX-Shimadzu model 720) was used to determine the concentration of the doping species, and the final glass composition.

3. Results

Fig. 1 shows TEM images corresponding to samples heat-treated for (a) 460, (b) 480, (c) 500, and (d) 540 °C.

From the EDX data the glass composition was determined (in wt.%) as 57.8PbO–33.2GeO_2–5.2Al_2O_3–3.8SiO_2. The concentration of the doping species was determined to be: 0.34 Tm_2O_3, 1.63 Yb_2O_3, and 1.77 Ag (in wt.%). Considering that the nominal values (in wt.%) are: 59.0 PbO, 41.0 GeO_2, 0.5 Tm_2O_3, 2.0 Yb_2O_3, and 1.9 Ag (originated from the addition of 3.0 $AgNO_3$), it is now noticed that the final composition presents Al_2O_3 and SiO_2 and both compounds are ascribed to originate from the alumina crucible and the quartz stick used in the preparation of the samples. This explains the differences between the nominal and experimental values.

Fig. 2 shows the optical absorption spectra of Tm^{3+}/Yb^{3+} codoped PGO samples containing silver NPs, heat-treated at 380, 420, 460, 480, 500, 520, and 540 °C for 6 h. The absorption bands associated to Tm^{3+} and Yb^{3+} ions are observed. A band in the range 400 to 500 nm related to the surface plasmon resonance (SPR) is also observed; the intensity of this band increases as the temperature of the heat-treatment is increased. The band position shifts to the infrared region, which is clearly visualized for the sample heat-treated at 540 °C.

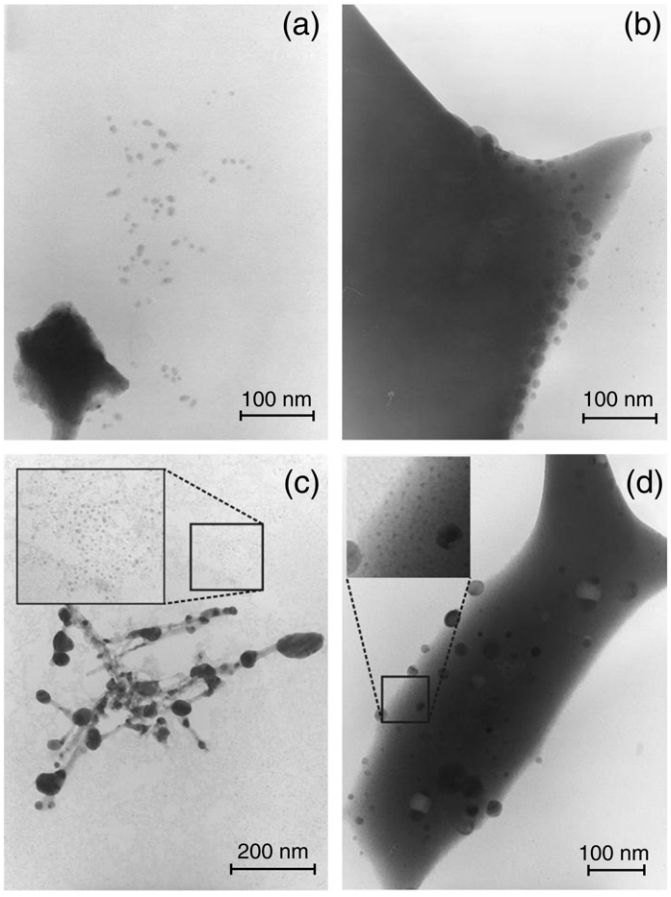

Fig. 1. Transmission electron microscope images of samples heat-treated at (a) 460, (b) 480, (c) 500 and (d) 540 °C.

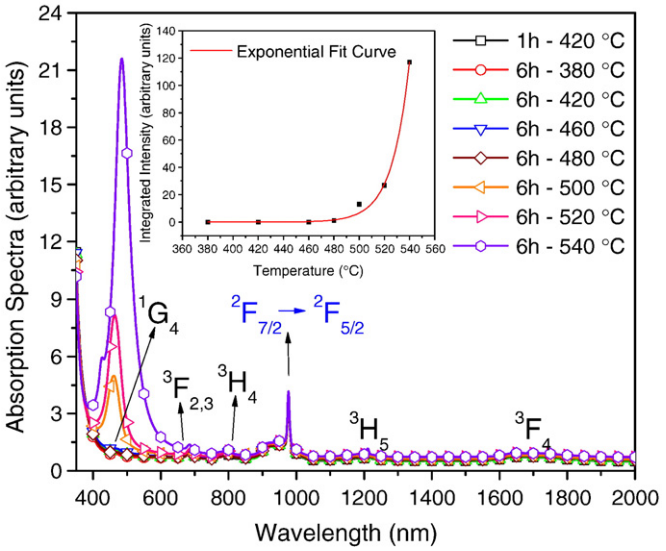

Fig. 2. Optical absorption spectra of Tm^{3+}/Yb^{3+} codoped PbO–GeO_2 samples containing silver NPs nucleated at different temperatures. The inset shows the integrated absorption intensity of the surface plasmon resonance band as a function of the temperature T_h.

Fig. 3 shows the UC emission spectra of Tm^{3+} ions for samples heat-treated at different values of T_{ht}. The emission bands centered in 455, 480, and 650 nm, correspond to the $^1D_2 \rightarrow {}^3F_4$, $^1G_4 \rightarrow {}^3H_6$, and $^1G_4 \rightarrow {}^3F_4$ transitions, respectively. Fig. 4 presents a simplified energy level diagram of Tm^{3+} and Yb^{3+} ions and describes the excitation pathways and the luminescence transitions. The mechanism of the UC for each transition was already discussed in ref. [20]. The first excitation step is due to the optical absorption by Yb^{3+} ions ($^2F_{7/2} \rightarrow {}^2F_{5/2}$ transition). Afterwards a multistep excitation occurs in the Tm^{3+} ions due to energy transfer from the excited Yb^{3+} ions.

4. Discussion

According to Fig. 1, the nucleated silver NPs have an average diameter of ≈7 nm for T_{ht} = 460 °C (Fig. 1a), ≈8 nm for T_{ht} = 480 °C (Fig. 1b), ≈5 nm for T_{ht} = 500 °C and 540 °C (Fig. 1c and d). For samples heat-treated above 500 °C it is observed a low concentration of NPs with average diameter around 30 nm. It was also observed that

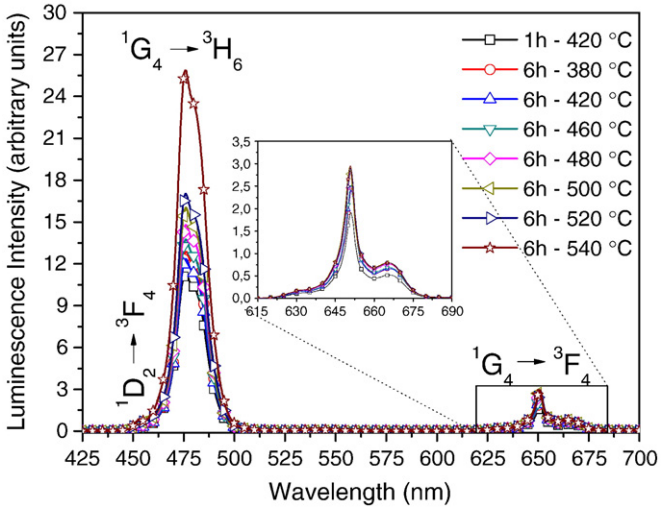

Fig. 3. Luminescence spectra of Tm^{3+}/Yb^{3+} codoped PbO–GeO_2 samples containing silver NPs (excitation at 980 nm).

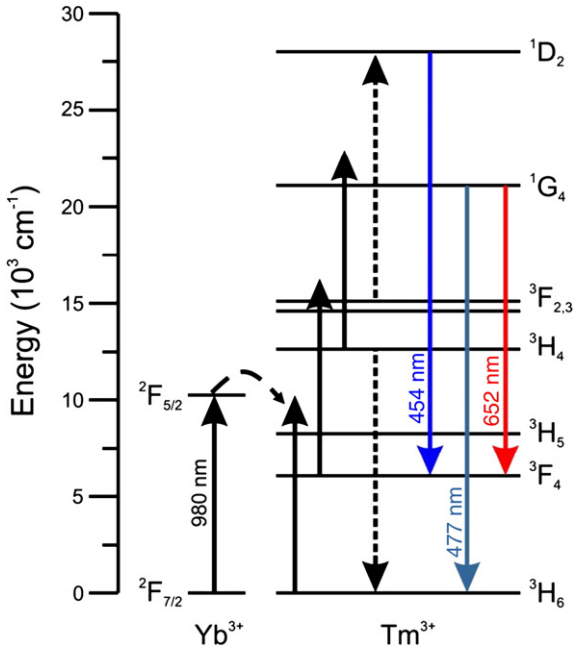

Fig. 4. Simplified energy level diagram of Tm^{3+}/Yb^{3+} ions with indication of the luminescence observed and the luminescence pathway.

the shape of the silver NPs does not change significantly with the increase of T_{ht}. The particle sizes were determined by measuring each individual particle observed in the micrographs with the by using the softwares Corel Draw and Origin for image and data processing, respectively. The dark regions in Fig. 1a, b and d represent the glass matrix with the silver nanoparticles embedded. The prominent dark structure in Fig. 1c represents the largest nanoparticles with diameter around 30 nm.

As previously reported in the literature [21], silver ions in glasses are very mobile and have the tendency to aggregate. So, NPs of various sizes can coexist, as heat-treatments are barely selective.

The absorption band related to the SPR was not observed for samples heat-treated below 500 °C, in Fig. 2, because the amount of nucleated silver NPs is not enough to present a noticeable effect, as previously reported [17]. Based on the dielectric function of silver [22] and the refractive index of the PGO glasses (≈2.0) it is estimated that the wavelength of surface plasmon resonance (λ_{SPR}) is located in the range of 400 to 500 nm. For samples heat-treated at 500 and 520 °C, the SPR band is centered at ≈460 nm. For samples heat-treated at 540 °C, it is observed a small shift of the band position towards the infrared region and a band centered at ≈490 nm. The inset in Fig. 2 shows a nonlinear dependence of the SPR absorption with T_h due to the increase of the NPs concentration.

Fig. 3 shows that the highest enhancement of luminescence occurs for the blue emission (480 nm). Considering that the wavelength of this transition ($^1G_4 \rightarrow {}^3H_6$) is close to the λ_{SPR}, this effect was already expected, and it can be attributed to the enhancement of the local field effect in the proximity of silver NPs. Notice that the luminescence band centered at 650 nm, corresponding to $^1G_4 \rightarrow {}^3F_4$ does not change much due to the large frequency detuning with respect to the SPR. The inset of Fig. 2 shows the enhancement of the emission at 650 nm related to the increase of the heat-treatment temperature.

Clearly the heat-treatments performed at higher temperatures favor the NPs nucleation, as corroborated by the three techniques used (optical absorption, TEM and UC luminescence).

5. Conclusions

Silver NPs were nucleated in lead germanate glasses submitted to suitable heat-treatments. Parameters to characterize the growth process were given. As the heat-treatment temperature is raised, the concentration of NPs increases, which is an evidence of the increase of the SPR absorption band. The heat-treatment temperature affects the nucleation of silver NPs and consequently the blue–red luminescence of Tm^{3+}/Yb^{3+} codoped PGO glasses upon excitation at 980 nm. The intensity of the UC luminescence at 480 nm is more influenced than the emission at 650 nm because of the proximity with the SPR. The enhanced UC emission in the visible region is attributed to the local field effect in the proximity of silver NPs combined with the $Yb^{3+} \rightarrow Tm^{3+}$ energy.

Acknowledgements

The authors thank CNPq (Conselho Nacional de Desenvolvimento Científico e Tecnológico for the financial support and Photonic National Institute of Science and Technology. This work was performed under the Nanophotonics Network Project.

References

[1] P.N. Prasad, Nanophotonics, Wiley, New York, 2004.
[2] M. Yamane, Y. Asahara, Glasses for Photonics, Cambridge University Press, Cambridge, 2000.
[3] V.A. Shneidman, Phys. Rev. Lett. 101 (2008) 205702.
[4] G. Nicotra, et al., J. Appl. Phys. 95 (2004) 2049.
[5] C. Strohhöfer, A. Polman, Appl. Phys. Lett. 81 (2002) 1414.
[6] J. Kalkman, L. Kuipers, A. Polman, H. Gersen, Appl. Phys. Lett. 86 (2005) 041113.
[7] Chiasera, et al., Opt. Mater. 27 (2005) 1743.
[8] F. Stellacci, et al., Adv. Mater. 14 (2002) 194.
[9] S.K. Mahapatra, et al., Nanotechnology 18 (2007) 135602.
[10] N.H. Ma, et al., Mater. Lett. 63 (2009) 151.
[11] S. Qu, et al., Chem. Phys. Lett. 368 (2003) 352.
[12] P. Nacharov, N.V. Nikonorov, A.I. Sidorov, V.A. Tsekhomskii, Glass Phys. Chem. 34 (2008) 693.
[13] M.B. Silva, C.B. de Araujo, S.S. Silva, A. Galembeck, J. Phys. Chem. Sol. 68 (2007) 729.
[14] L.R.P. Kassab, C.B. de Araújo, Germanate and tellurite glasses for photonic applications, Photonics Research Developments, Nova Science Publishers, New York, 2008, pp. 385–409, Chapter 13.
[15] L.P. Naranjo, C.B. de Araújo, O. Malta, P.S. Cruz, L.R.P. Kassab, Appl. Phys. Lett. 87 (2005) 241914.
[16] D.M. da Silva, L.R.P. Kassab, S.R. Lüthi, C.B. de Araújo, A.S.L. Gomes, M.J.V. Bell, Phys. Lett. 90 (2007) 081913.
[17] L.R.P. Kassab, F.A. Bonfim, J.R. Martinelli, N.U. Wetter, J.J. Neto, C.B. de Araújo, Appl. Phys. B Lasers Opt. 94 (2008) 239.
[18] L.R.P. Kassab, D.S. da Silva, R.A. Pinto, C.B. de Araújo, Appl. Phys. Lett. 94 (2009) 101912.
[19] L.A. Gomez, F.E.P. Santos, A.S.L. Gomes, C.B. de Araújo, L.R.P. Kassab, W.G. Hora, Appl. Phys. Lett. 92 (2008) 141916.
[20] T.A.A. de Assumpção, D.M. da Silva, L.R.P. Kassab, C.B. de Araújo, J. Appl. Phys. 106 (2009) 063522.
[21] M. Mattarelli, M. Montagna, K. Vishnubhatla, A. Chiasera, M. Ferrari, G.C. Righini, Phys. Rev. B 75 (2007) 125102.
[22] E.D. Palik, Handbook of Optical Constants of Solids, Academic, New York, 1985.